34th Annual International Conference of the IEEE EMBS
San Diego, California USA, 28 August - 1 September, 2012

Multi-Push (MP) Acoustic Radiation Force (ARF) Ultrasound for Assessing Tissue Viscoelasticity, *In Vivo**

Mallory R. Scola, Leslie M. Baggesen, and Caterina M. Gallippi, *Member, IEEE*

Abstract— **Acoustic radiation force (ARF) ultrasound is a method of elastographic imaging in which micron-scale tissue displacements, induced and tracked by ultrasound, reflect clinically relevant tissue mechanical properties. Our laboratory has recently shown that tissue viscoelasticity is assessed using the novel Multi-Push (MP) ARF method. MP ARF applies the Voigt model for viscoelastic materials and compares the displacements achieved by successive ARF excitations to qualitatively or quantitatively represent the relaxation time for constant stress, which is a direct descriptor of the viscoelastic response of the tissue. We have demonstrated MP ARF in custom viscoelastic tissue mimicking materials and implemented the method *in vivo* in canine muscle and human renal allografts, with strong spatial correlation between MP ARF findings and histochemical features and previously reported mechanical changes with renal disease. These data support that noninvasive MP ARF is capable of clinically relevant assessment of tissue viscoelastic properties.**

I. Introduction

Physicians have long used palpation as a simple diagnostic tool for detecting differences in the mechanical properties of tissue and identifying abnormalities. The mechanical properties of tissue vary widely among different physiological and pathological states[1] and thus have significant diagnostic potential. For instance, the relative hardness of malignant tumors is the basis for the use of palpation to detect breast cancer.[2] However, palpation is only applicable to superficial organs and pathologies and is subjective and limited to the touch sensitivity of the practioner.

In recent decades, significant effort has been directed towards producing techniques for non-invasive characterization of the mechanical properties of tissue. Elastography methods are generally based on inducing tissue deformation or displacement and detecting the response.[3, 4] One established ultrasonic method for noninvasively interrogating the mechanical properties of tissue is Acoustic Radiation Force Impulse (ARFI) imaging. In ARFI imaging a short duration and relatively high intensity acoustic impulse is used to generate localized displacements in a given region of excitation.[5, 6] The region of excitation is translated across the imaging field of view. An extensive body of literature documents the wide relevance of ARFI-based methods in clinical diagnostic imaging; however these applications have primarily focused on the elastic properties of tissue and have neglected tissue viscosity. The omission of viscosity can cause error in the estimation of tissue elasticity;[7] moreover, important information about the physiological state of the tissue may be lost.

Viscoelastic properties may be assessed by a variety of acoustic methods. Some approaches relate viscoelastic properties to shear wave propagation characteristics.[8-13] Other approaches apply sustained mechanical force to solve for elastic and viscous parameters using established viscoelastic models. In quasistatic elastography, viscoelastic features can be recovered from time-varying strain[14]. A compression-hold-release stress stimulus can be used to form images of elastic strain and strain delay times. However, very long acquisition times (>100 s) are necessary to get this information, making the *in vivo* relevance limited. Kinetic Acoustic Vitreoretial Examination (KAVE)[15] and Monitored Steady-State Excitation and Recovery (MSSER)[16] both use multiple successive ARF impulses to fully displace tissue and solve for viscoelastic properties by fitting experimental displacement to the Voigt or standard linear viscoelastic models. Because these methods require that tissue achieve steady-state displacement, KAVE and MSSER suffer from slow frame rate and/or tissue heating from the amplitude and duration of ARF excitations necessary in physiologically relevant conditions.

Multi-Push (MP) Acoustic Raditation Force (ARF) ultrasound is a novel approach to assessing tissue viscoelasticity in which two successive ARF excitations are used to estimate viscoelastic parameters.[17] In this manuscript, we describe the theory underlying MP ARF and review its performance in tissue mimicking materials, canine muscle *in vivo*, and human renal allografts *in vivo*.

II. Background

A. The Voigt Model

The mechanical properties of soft tissue have been widely studied in the field of biomechanics with several viscoelastic models describing tissue response to mechanical stimuli. The Voigt model describes tissue displacement in response to a unit step forcing function of magnitude A and duration t_{ARF} as

$$PD_1 = \frac{A}{E\mu}\left(1 - e^{-t_{ARF}/\tau_\sigma}\right) \quad (1)$$

where $E\mu$ is the relaxed elastic modulus and τ_σ is the relaxation time constant (RTC) for constant stress = η / $E\mu$, where η is the coefficient of viscosity.[16]

B. Multi-Push (MP) Acoustic Radiation Force (ARF)

MP ARF exploits the Voigt model to assess the viscoelastic properties of tissue.[17] By applying two

successive ARF excitations in the same region of excitation, three points along the displacement profile described in (1) are observed. The relative shape of the displacement profile, which reflects τ_σ, can be described qualitatively using the parameter marginal peak displacement (MPD), where

$$MPD = (PD_2 - D) / PD_1. \quad (2)$$

The displacements achieved by the first and second ARF excitations are PD_1 and PD_2, respectively, and D is the displacement remaining from the first excitation at the time of the second excitation. Tissues that recover nearly fully from the first excitation before the second excitation is administered will have a small D, and PD_2 will approximately equal PD_1, yielding $MPD \approx 1$. This response is expected for elastic tissue with low viscosity. Tissues with relatively low elasticity and high viscosity will experience little recovery by the time of the second push, yet still be far from steady state, resulting in a large difference between PD_2 and D relative to PD_1 and an MPD that is <1. Tissues with both relatively high elasticity and high viscosity will be at or nearing steady-state following the first push. Since this tissue will have experienced little recovery by the time of the second push, the difference between PD_2 and D will be small relative to PD_1, yielding a small MPD.

While MPD discriminates viscoelastic tissue properties, it is not quantitative. Quantitative assessment of tissue viscoelasticity may be achieved in MP ARF by considering again the Voigt model. After allowing a short time for partial recovery from the first ARF excitation, the displacement remaining is D, and thus the displacement following the second ARF excitation is predicted as,

$$PD_2 = \frac{A}{E\mu} - \left(\frac{A}{E\mu} - D\right) e^{-t_{ARF}/\tau_\sigma} \quad (3)$$

Subtracting (1) from (2) and solving for the RTC yields,

$$\tau_\sigma = \frac{-t_{ARF}}{\ln\left(\frac{PD_2 - PD_1}{D}\right)} \quad (4)$$

In other words, using MP ARF, the ratio of the coefficient of viscosity to the relaxed elastic modulus can be directly calculated.

III. Methods

A. MP ARF Imaging Methods

MP ARF imaging was performed in viscoelastic tissue mimicking materials and *in vivo in* normal canine muscle and human renal allografts. Applicable procedures and protocols were in accordance with institutional guidelines and approved by the UNC-IACUC and the UNC-IRB. Imaging was conducted using a Siemens ACUSON or Sonoline Antares imaging system equipped for research purposes and a VF7-3 transducer (Siemens Medical Solutions USA Inc, Ultrasound Division). The two MP ARF excitations were 300 cycles in duration and centered at 4.21 MHz with an F/1.5 focal configuration. The time separation between the two ARF excitations was 0.8 ms. Both ARF excitations were followed by two-cycle tracking beams centered at 6.15 MHz with an 11 kHz PRF. Axial displacements were calculated from the tracking lines using one-dimensional cross-correlation.[18] MPD and RTC were calculated using (2) and (4), respectively, and the corresponding parametric images were rendered.

B. Viscoelastic Tissue Mimicking Materials

Five homogeneous, agar/gelatin tissue mimicking phantoms were prepared with different concentrations of gelation to vary elasticity and different concentrations of xanthan gum to alter viscosity.[19] A structured agar/gelatin phantom was also constructed with a background of high elasticity and low viscosity and a lesion of comparable elasticity and increased viscosity. For each homogenous phantom, MP ARF imaging was implemented to calculate RTC. As a validadation standard, elasticity and viscosity were characterized using Shear wave Dispersion Ultrasound Vibrometry (SDUV)[20] and corroborated with Shear Wave Spectroscopy.[21]

B. Canine Muscle, In Vivo

MP ARF imaging was performed *in vivo* in the semitendinosus muscle of a golden retriever crossbred dog with no known muscle pathologies. The MP ARF imaging plane was marked with a methylene blue injection using B-Mode guidance, and the corresponding muscle cross-section was removed following necropsy. The excised muscle was then sectioned and stained with hematoxylin and eosin, Masson's trichrome and oil red o.

C. Human Renal Transplants

MP ARF imaging was performed in the transplanted kidneys of 44 renal allograft recipients.[22] Imaging results in control subjects (for whom biopsy was not clinically indicated due to low likelihood of graft disease, n=25) were compared to results in subjects undergoing biopsy (with suspected likelihood of graft disease greater than 50%, n=19). Each biopsy patient was retrospectively grouped into disease categories according clinical pathologists' interpretations of biopsy results.

For each kidney, MPD was calculated in five distinct regions of interest (ROIs), located within 5 mm above the imaging focal depth. The ROIs were positioned at: the outer edge of the parenchyma, the center of the parenchyma, the inner edge of the parenchyma (bordering on the pelvis), the outer edge of the pelvis (bordering on the parenchyma), and an inner region in the pelvis. The ratios of MPD between all ROIs were then calculated and compared across diagnostic categories (for example, MPD in the outer edge of the parenchyma : MPD in the outer edge of the pelvis in acute rejection was compared to MPD in the outer edge of the parenchyma : MPD in the outer edge of the pelvis in controls). Statistically significant differences were determined using the two-sample Wilcoxon test (Mann-Whitney test) at 95% confidence level.

IV. Results and Discussion

A. Viscoelastic Tissue Mimicking Materials

Average RTC values and the corresponding reference value calculated by SDUV are reported in Table 1. Results showed good agreement of RTC values calculated using MP ARF with those calculated with SDUV and demonstrate the relevance of the RTC calculations. The parametric image of RTC in the structured phantom (fig 1) discriminated the viscous lesion with a contrast-to-noise (CNR) of 1.2, whereas conventional ARFI peak displacement showed contrast of the lesion from the background with a CNR of 0.09.

Table 1. RTC measurements in tissue mimicking phantoms

RTC (ms)	SDUV (ms)
0.062 ± 0.019	0.068 ± 0.013
0.074 ± 0.018	0.074 ± 0.006
0.076 ± 0.032	0.076 ± 0.003
0.081 ± 0.028	0.088 ± 0.005
0.091 ± 0.015	0.121 ± 0.016

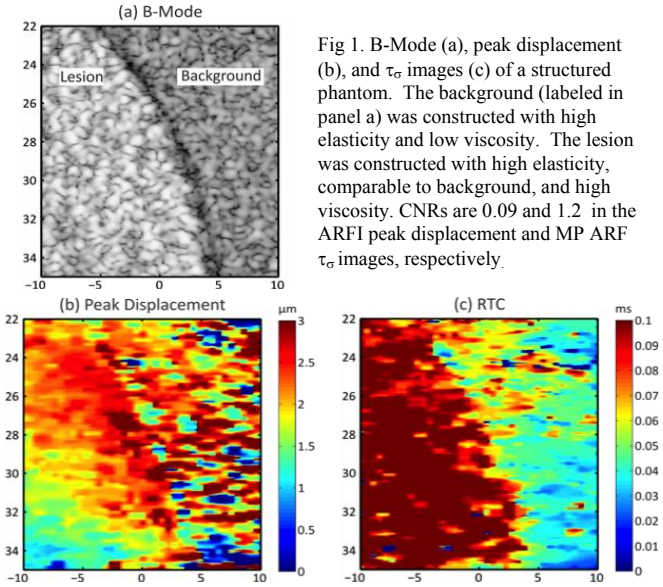

Fig 1. B-Mode (a), peak displacement (b), and τ_σ images (c) of a structured phantom. The background (labeled in panel a) was constructed with high elasticity and low viscosity. The lesion was constructed with high elasticity, comparable to background, and high viscosity. CNRs are 0.09 and 1.2 in the ARFI peak displacement and MP ARF τ_σ images, respectively.

B. Normal Canine Muscle, In Vivo

Figure 2 shows the B-Mode image, spatially matched gross anatomy, RTC image, and histology. The RTC image (panel e) shows an area with high RTC (circled) suggesting low elasticity and/or high viscosity. The oil red o stained section (panel j) indicates that this area corresponds to a fat deposit, which supports high τ_σ. The RTC images also shows alignment of echogenic structures to regions of low RTC indicating high elasticity or low viscosity. The Masson's trichrome stained section (panel i) shows that the highlighted tissue structures are composed of collagen, which supports lower τ_σ values. We have previously reported focal regions of low MPD in areas of fibrous deposition (corroborated by B-Mode and MRI) and true hypertrophy (corroborated by myofiber cross-sectional area measurements) in dystrophic canine muscle.[23] The results are not discussed here for brevity.

C. Human Renal Allografts, In Vivo

In cases of moderate vascular disease, the MPD ratios of center parenchyma : inner pelvis, inner edge of parenchyma : inner pelvis, and inner pelvis : outer edge of pelvis were significantly different compared to the same ratios of MPD values from non-biopsied patient volunteers ($p = 0.0118$, 0.0256, and 0.0256, respectively). The ratios from the disease state were consistently higher than those in the control group; this indicates that the inner pelvis has consistently smaller MPD values than the center parenchyma, the inner edge of the parenchyma, and the outer edge of the pelvis in moderate vascular disease than in controls. If the inner pelvis is largely spared in renal disease and is softer than the parenchyma[24] in healthy states, this suggests that the center parenchyma, inner parenchyma, and outer parenchyma become softer and/or less viscous in moderate vascular disease. Greater detail is provided in [22]. This finding is consistent with previously reported softening of the renal parenchyma with reduced perfusion, as is expected in moderate vascular disease. The fact that statistically significant differences in MPD were not detected in severe vascular disease versus control is in agreement with prior reports that fibrosis masks the softening effects of reduced perfusion in advanced vascular disease. [25]

V. Conclusion

MP ARF is a novel method for noninvasively describing the viscoelastic property of tissue. Using two successive ARF excitations delivered in the same region of excitation, MP ARF solves for the relaxation time constant (RTC) for constant stress, which is defined as the ratio of the coefficient of viscosity to the relaxed elastic modulus in the Voigt biomechanical model. MP ARF has been validated in viscoelastic tissue mimicking materials, demonstrated in canine muscle *in vivo* with strong spatial correlation to histochemical features, and demonstrated in human renal allografts *in vivo* with agreement to previously reported mechanic changes in renal parenchyma with moderate vascular disease. These data strongly support the clinical relevance of viscoelastic property imaging by MP ARF ultrasound.

Acknowledgment

We thank Siemens Medical Solutions, USA Inc. Ultrasound Division for technical support.

References

[1] Sarvazyan AP, Rudenko OV, Swanson SD, et al. Shear wave elasticity imaging: A new ultrasonic technology of medical diagnostics, *Ultrasound in medicine & biology 24,* 1419-1435 (1998).

[2] Barton MB, Harris R, and Fletcher SW. The rational clinical examination. Does this patient have breast cancer? The screening clinical breast examination: Should it be done? How?, *JAMA : the journal of the American Medical Association 282,* 1270-1280 (1999).[3] Greenleaf JF, Fatemi M, and Insana M. Selected methods for imaging elastic properties of biological tissues, *Annu Rev Biomed Eng 5,* 57-78 (2003).

[4] Gao L, Parker KJ, Lerner RM, et al. Imaging of the elastic properties of tissue--a review, *Ultrasound in medicine & biology 22,* 959-977 (1996).

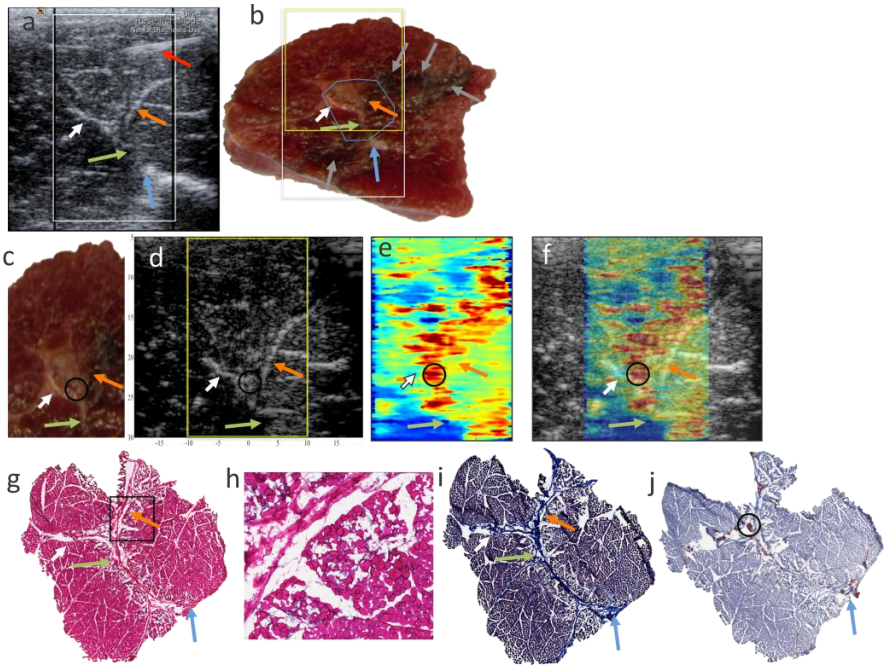

Fig. 2: Alignment of B-Mode, gross anatomy, RTC, and histology images in control dog ST. Panel a: screen-grab of B-Mode image with echogenic tissue structures highlighted (yellow, orange, green, and blue arrows) and injection needle visible (red arrow). Panel b: Gross image of ST cross-section aligned to B-Mode image with tissue structures appearing in B-Mode image highlighted (yellow, orange, green, and blue arrows, respectively) and macroscopically visible methylene blue stain (gray arrows); the MP ARF imaging (yellow box) and histological (blue polygon) fields of view. Panel C: gross image zoomed to the MP ARF imaging FOV. Panel D: B-Mode image reconstructed from MP ARF data, with MP ARF FOV (yellow lines) and tissue structures highlighted (yellow, orange and green arrows). Panel E: Corresponding RTC image. Panel F: B-Mode with transparent RTC. Panels g-j: matched histochemistry of H&E (g) with higher magnification to show methylene blue (h), Masson's trichrome (i), and oil red o (j).

[5] Nightingale K, Soo MS, Nightingale R, et al. Acoustic radiation force impulse imaging: In vivo demonstration of clinical feasibility, *Ultrasound in medicine & biology 28,* 227-235 (2002).

[6] Palmeri ML, McAleavey SA, Fong KL, et al. Dynamic mechanical response of elastic spherical inclusions to impulsive acoustic radiation force excitation, *IEEE transactions on ultrasonics, ferroelectrics, and frequency control 53,* 2065-2079 (2006).

[7] Bercoff J, Tanter M, Muller M, et al. The role of viscosity in the impulse diffraction field of elastic waves induced by the acoustic radiation force, *IEEE transactions on ultrasonics, ferroelectrics, and frequency control 51,* 1523-1536 (2004).

[8] Catheline S, Gennisson JL, Delon G, et al. Measurement of viscoelastic properties of homogeneous soft solid using transient elastography: An inverse problem approach, *J Acoust Soc Am 116,* 3734-3741 (2004).

[9] Chen SG, Fatemi M, and Greenleaf JF. Quantifying elasticity and viscosity from measurement of shear wave speed dispersion, *J Acoust Soc Am 115,* 2781-2785 (2004).

[10] Chen S, Urban MW, Pislaru C, et al. Shearwave dispersion ultrasound vibrometry (sduv) for measuring tissue elasticity and viscosity, *IEEE transactions on ultrasonics, ferroelectrics, and frequency control 56,* 55-62 (2009).

[11] Bercoff J, Tanter M, and Fink M. Supersonic shear imaging: A new technique for soft tissue elasticity mapping, *IEEE transactions on ultrasonics, ferroelectrics, and frequency control 51,* 396-409 (2004).

[12] Tanter M, Bercoff J, Athanasiou A, et al. Quantitative assessment of breast lesion viscoelasticity: Initial clinical results using supersonic shear imaging, *Ultrasound in medicine & biology 34,* 1373-1386 (2008).

[13] Muller M, Gennisson JL, Deffieux T, et al. Quantitative viscoelasticity mapping of human liver using supersonic shear imaging: Preliminary in vivo feasability study, *Ultrasound in Medicine and Biology 35,* 219-229 (2009).

[14] Insana MF, Pellot-Barakat C, Sridhar M, et al. Viscoelastic imaging of breast tumor microenvironment with ultrasound, *J Mammary Gland Biol 9,* 393-404 (2004).

[15] Walker WF, Fernandez FJ, and Negron LA. A method of imaging viscoelastic parameters with acoustic radiation force, *Phys Med Biol 45,* 1437-1447 (2000).

[16] Mauldin FW, Jr., Haider MA, Loboa EG, et al. Monitored steady-state excitation and recovery (msser) radiation force imaging using viscoelastic models, *IEEE transactions on ultrasonics, ferroelectrics, and frequency control 55,* 1597-1610 (2008).

[17] Scola MR, Gallippi CM. "Multi-Push (MP) ARF Assessment of Viscoelastic Properties in a Tissue Mimicking Phantom," in *Ultrasonics Symposium (IUS), 2011 IEEE*, 2011.

[18] Pinton GF, Dahl JJ, and Trahey GE. Rapid tracking of small displacements with ultrasound. *IEEE Transactions on UFFC.* 53, no. 6 (2006): 1103–17.

[19] Vappou J, Maleke C, and Konofagou EE. Quantitative viscoelastic parameters measured by harmonic motion imaging, *Phys Med Biol 54,* 3579-3594 (2009).

[20] Mitri FG, Urban MW, Fatemi M, et al. Shear wave dispersion ultrasonic vibrometry for measuring prostate shear stiffness and viscosity: An in vitro pilot study, *IEEE transactions on bio-medical engineering 58,* 235-242 (2011).

[21] Deffieux T, Montaldo G, Tanter M, et al. Shear wave spectroscopy for in vivo quantification of human soft tissues visco-elasticity, *IEEE Trans Med Imaging 28,* 313-322 (2009).

[22] Scola MR, Baggesen LM, Wu CD et al. Clinical Multi-Push Acoustic Radiation Force for Evaluation of Renal Transplant Status. *Proceedings IEEE International Ultrasonic Symposium* (2011).

[23] Scola MR, Kornegay JN, Gallippi CM. "Acoustic radiation force assesessment of muscular mechanical properties in a crossbred dystrophin-deficient, myostatin-null canine model" (presented at the Ultrasonic Imaging and Tissue Characterization Symposium, Arlington, VA, 2010).

[24] Arda K, Ciledag N, Aktas E, Anbas BK, Kose K. "Quantitative Assessment of Normal Soft-Tissue Elasticity Using Shear-Wave Ultrasound Elastography," *American Journal of Roentgenology* 197, no. 3 (2011): 532–536.

[25] Warner L, Meng Y, Glaser KJ, et al. Noninvasive In Vivo Assessment of Tissue Elasticity During Graded Renal Ischemia Using MR Elastography. Investigative Radiology 46(8):509-15.